Granular Matter (2022) 24:28
https://doi.org/10.1007/s10035-021-01186-3

ORIGINAL PAPER

On the contact problem of soft-rigid interfaces: incorporation of Mindlin-Deresiewicz and self-deformation concepts

Yu Tian[1] · **Kostas Senetakis**[1]

Received: 20 January 2021 / Accepted: 2 November 2021

Abstract
The contact problem of soft-rigid interfaces is investigated in this study performing micromechanical-based experiments on sand (rigid) grains sliding against granulated (soft) rubber and by incorporating the Mindlin-Deresiewicz model. The analysis suggested that modifications of the theoretical model are necessary by taking into account, quantitatively, the deformable nature of the soft particles in terms of self-deformations during sliding. Interface friction, tangential stiffness and microslip displacement are analyzed and an attempt is made to provide inter-correlations among different contact parameters, incorporating experimental stiffness and realistic displacement thresholds into the theoretical model.

Keywords Constitutive modeling · Composite interface · Micromechanics · Friction · Tangential stiffness · Microslip displacement

1 Introduction

Environmental issues related with the enormous disposal of wasted automobile tires in landfills have led the scientific and engineering communities to find effective solutions in recycling and beneficially reusing these materials most commonly in a shredded form in various projects including transportation, infrastructure and geotechnical engineering applications [1, 2]. Over the previous three decades, many researchers have investigated the properties of recycled automobile tires in shredded (and granular) form, pure as well as mixed with soils and many studies have indicated promising applications in ground treatment and enhancement of soil mechanical behavior [3–16]. This has also resulted in ASTM to issue specifications related with the use of recycled shredded/granulated rubber in infrastructure projects [17, 18]. Sand-rubber mixtures are binary materials and their micromechanical behavior is represented by "soft-rigid" analog contacts. It is therefore important, in order to provide insights into their behavior, to further investigate the frictional mechanisms at the grain-scale between soil particle and rubber interfaces, which may contribute to enhanced constitutive modeling of these complex materials.

In their multi-scale experimental study on granulated rubber-sand composites, Li et al. [15] reported a direct relationship between bulk strength at the critical state and inter-particle friction angle. Insights into the behavior of these complex (composite) materials have also been observed through discrete-based numerical simulations, for example using the discrete element method (DEM), which allows an investigation into the load transfer and the dominant (micro-)mechanisms controling the response of binary and composite mixtures. Multi-scale integrated experimental and numerical works have also contributed to the state-of-the-art literature with respect to the behavior of binary and composite materials [6, 14, 19–26]. For example, Lopera Perez et al. [20] investigated, through DEM analyses, the influence of relative sizes of rubber and sand grains on the small-to-medium strain mechanical behavior of binary mixtures and they reported a positive contribution of the deviatoric stress to the behavior of the binary material through the more prevalent contribution of the sand-rubber contacts when rubber size increased. Lopera Perez et al. [21] further reported that the stability of sand-rubber binary mixtures was contributed by the interplay between sand-rubber and sand-sand contacts. Such a contribution was related to the positive (or negative) relationship between contact development and

✉ Kostas Senetakis
ksenetak@cityu.edu.hk

Yu Tian
ytian52-c@my.cityu.edu.hk

[1] Department of Architecture and Civil Engineering, City University of Hong Kong, Hong Kong, China

Published online: 15 December 2021

deviatoric stress influencing the normal contact force anisotropy and varied with rubber fraction. These numerical results showed a qualitative agreement with the experimental studies by [7, 27, 28] on that the content of rubber and the relative size of sand against rubber particles are two key factors in assessing the dominant mechanisms which control the behavior of these binary materials as the preferable response is the one that corresponds to sand-dominant or sand-rubber transitional zone of behavior, rather than rubber-dominant behavior.

The importance of the contact and frictional behavior of interfaces as well as grain morphological and elastic characteristics on the bulk constitutive response of granular materials has been acknowledged by many researchers through experimental works [15, 29–31] and theoretical/numerical studies [32–41], or combining advanced testing with computer simulations [42, 43]. The coefficient of interparticle friction (μ), which, in turn, is affected by material type and morphology, influences the dilation behavior, the bulk strength and the energy dissipation of particulate materials. Contact mechanics studies have also analytically investigated and/or modeled the problem of interacting bodies in the presence of rough surfaces [44–48].

Despite the enhancements in the state-of-the-art knowledge from micromechanical-based discrete simulations and contact mechanics model development investigating the grain-scale and multi-scale behavior of granular matter, less progress was reported over the previous decades on the experimental micromechanical response of granular materials. This would be particularly useful in the analysis of granular materials which display strong interlinks between micro- and macro-scale responses [49–53]. New generation of laboratory setups were presented in recent years, which allowed the experimental investigation into the contact problem of powders and grains with applications in studies of geomechanics and engineering geology problems, petroleum engineering as well as in fundamental studies in physics and mechanics disciplines [29, 54–61]. Based on this, significant progress was reported in recent years on the tribological behavior of natural soil grains and other natural or engineered interfaces and many studies [86, 87, 93, 94] emphasized on the important influence of surface roughness, morphology at the small-to-meso scale, hardness and Young's modulus on the interface friction and tangential load—displacement (constitutive) behavior of contacted bodies [62–64]. Following the experimental configuration presented by Senetakis and Coop [55], He et al. [60] developed an apparatus which provided insights into the friction-shearing velocity relationship for sand and sand-rubber composite contacts, which study also reported on the energy dissipation of binary materials.

Rubber in granulated or shredded form, comprises an excellent composite for treatment of weak soils such as chemically weathered rocks which have very crushable grains as the addition of soft rubber granules mitigates sand grain breakage contributing to the reduction of settlements [15, 16]. Thus, on a practical standpoint, ground treatment with rubber may provide beneficial solutions in improving the performance of engineered soils. Because of their high energy dissipation capacity, rubber has also been proposed and examined through laboratory research works and theoretical studies to be used as an alternative and of low-cost seismic isolation measure for superstructures and earth systems [28, 65].

Understanding the fundamental mechanisms contributing to the bulk behavior of binary materials, such as sand-rubber mixtures, necessitates more systematic studies to be performed at the grain-scale. An important aspect of this is the evaluation of the applicability of contact mechanics models, commonly used in the simulation of discrete materials, on the performance of soft-rigid types of contacts. In the present work, a comprehensive grain-scale laboratory research was carried out investigating the tribological behavior of sand-rubber composite interfaces using two different types of natural sand; a benchmark quartz-type sand and grains from a saprolite extrusive igneous rock. The emphasis of the study was placed on both the frictional response (interparticle coefficient of friction) and the constitutive behavior of the composite interfaces in terms of tangential (or shearing) force—displacement relationship, which can provide quantification of contact stiffness. All these parameters are important to be obtained from experimental observations in order to constitute a basis for discrete-based numerical input parameters as well as to understand at the fundamental level of grain-scale the differences in the responses between binary interfaces in which different sand types are used.

2 Methodology

2.1 Material description and testing apparatus

The grain-scale (interface) experiments were performed with a custom-built micromechanical apparatus [55, 58, 62]. A schematic illustration of the experimental setup is given in Fig. 1.

The apparatus consists of two horizontal loading arms positioned orthogonally, and one axis positioned in the vertical direction. The inherent friction of the system is minimised by using a set of chrome steel balls beneath the guiding sled and frictionless linear guides equipped at the different mechanical connections of the apparatus. During the tests, one of the two horizontal systems applies the shearing at the contact of the grains, while the desired normal load is applied through the vertically positioned system; the second horizontally placed system is used, primarily,

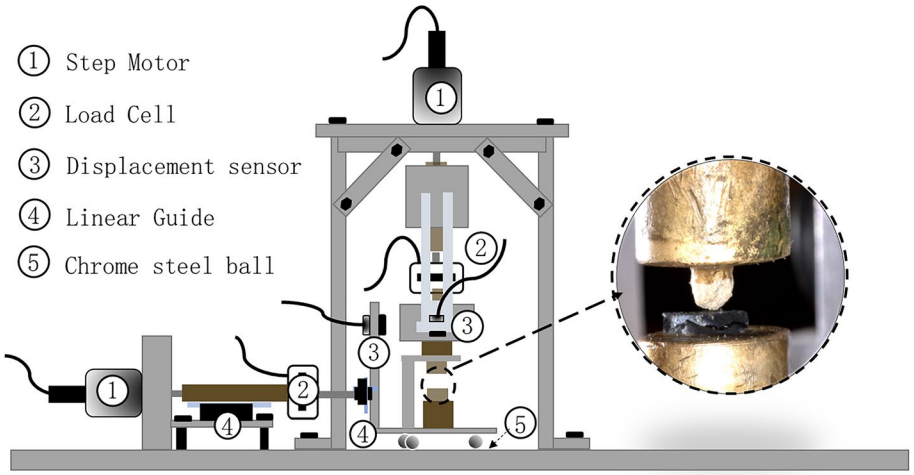

Fig. 1 Schematic diagram of the micromechanical testing setup

in maintaining the stability of the system in the out-of-plane direction, or the use of more complex loading paths. This experimental setup uses high precision load cells and non-contact displacement sensors as well as high quality amplifying and filtering systems allowing in this way the resolution of forces and displacements in a way that contact stiffness can be computed.

Micromechanical experiments were performed at the interfaces of rubber–sand specimens using particles of 2 to 5 mm in size. The rubber is produced from the shredding process of recycled tires. In the present study, the rubber is classified as "granulated rubber" based on ASTM specifications [17], and the polymeric grains selected for the experiments had relatively flat surfaces (resulting in zero local curvature, or infinite radius, in the vicinity of the contacts). For sand grains, two different materials were selected as: (1) Leighton Buzzard sand (LBS) and (2) completely decomposed volcanic grains (CDV). LBS consists of quartz grains with regular shape (i.e. relatively spherical and rounded grains) and smooth surface texture. This is a benchmark sand which has also been investigated in previous works [66, 67]. CDV is composed of weathered extrusive to shallow intrusive rock and it has formed a clay-type of coating on the surfaces of the grains because of the chemical weathering of the parent rock. Scanning electron microscopic (SEM) images of the different materials used in the study are given in Fig. 2. The roughness of both LBS and CDV has been assessed based on white-light interferometry measurements [66, 68], and the data are summarised in Table 1.

2.2 Testing program

Monotonic shearing tests were performed on two types of composite interfaces including: (1) LBS-rubber and (2) CDV-rubber and additional tests were performed on pure sand grains and pure rubber grains to assess their tribological properties, while the applied normal load (F_N) was equal to either 1 N or 2 N for each test (i.e. shearing for each sample was carried out at a constant normal load). In a granular assembly subjected to macroscopic stress, the normal force at each contact varies greatly in more than one order of magnitude, hence it's not feasible to specify the one-to-one relationship between normal load and external stress level. The normal load was so selected to be compared with benchmark values from previous micromechanical-based works [60, 69].The code names of the specimens are: (1) C-R-1 N (2) C-R-2 N (3) L-R-1 N (4) L-R-2 N to represent the different testing materials ("C": "CDV", "R": "rubber", L: "LBS") and the applied normal load (1 N or 2 N). For each type of composite interfaces, 20 pairs of grains were sheared monotonically at a velocity of 0.2 mm/h. Note that for pure sand specimens of LBS-LBS and CDV-CDV, the experiments were carried out at a shearing velocity of 0.1 mm/h and the shearing velocity was set to be 0.2 mm/h for rubber-rubber interfaces.

3 Results and discussion

3.1 Monotonic shearing of composite interfaces: General observations on friction

Representative plots of shearing force—displacement for different types of interfaces are given in Fig. 3 corresponding to 1 N of normal load and a summary of the whole set of experiments is given in Table 2 (for pure sand and pure rubber contacts) and Tables 3 and 4 (for composite interfaces of LBS-rubber and CDV-rubber). In these tables, μ represents the interface (interparticle) coefficient of friction, K_{T0} represents the initial tangential stiffness, and d_s represents the slip displacement.

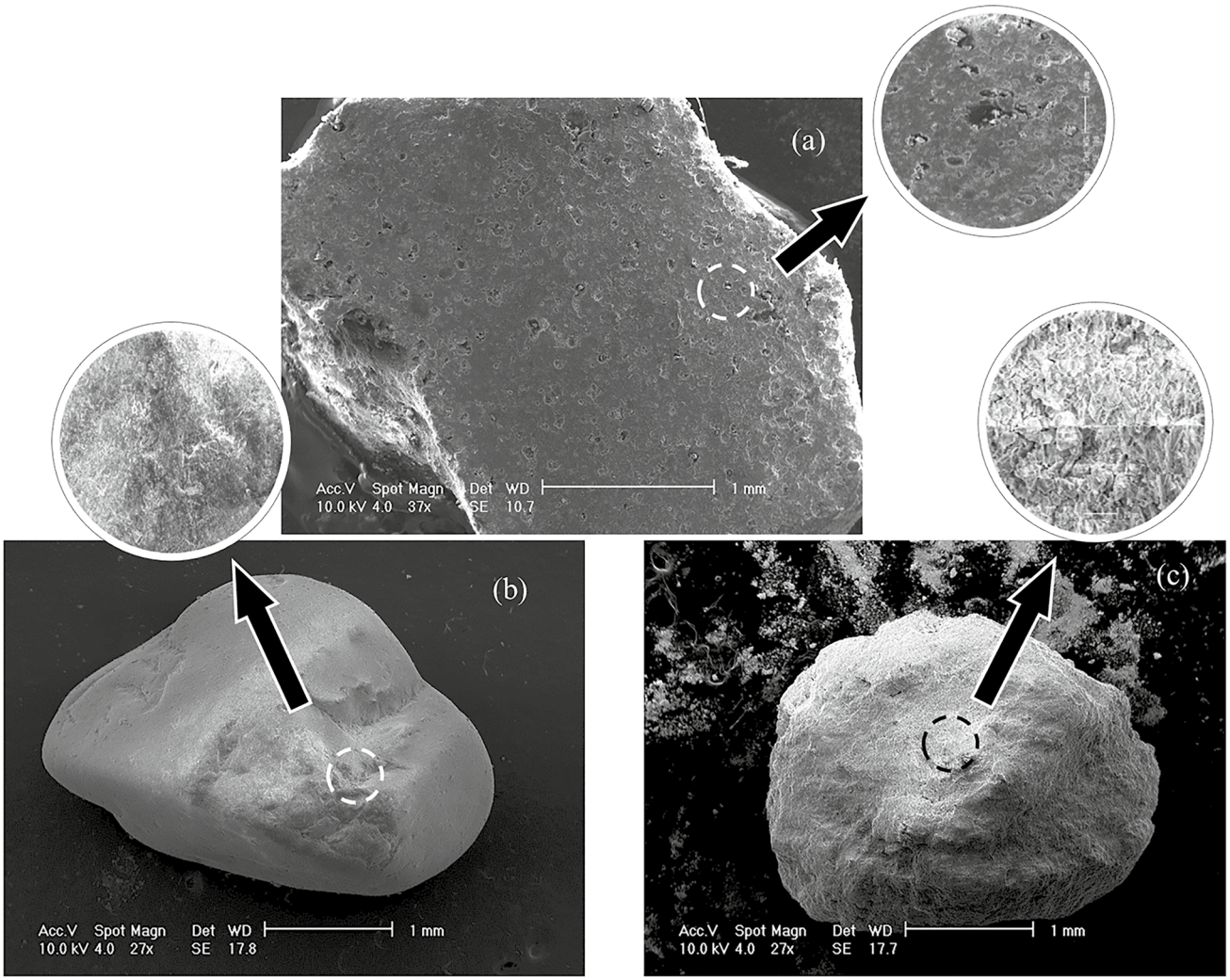

Fig. 2 SEM images of representative grains of **a** Rubber, **b** LBS and **c** CDV

Table 1 Representative roughness and hardness values of LBS and CDV particles

Material Code	Roughness (nm)	Hardness (GPa)
LBS [66]	223	4.9
CDV[68]	950	–

For pure LBS-LBS and CDV-CDV specimens, the interparticle coefficient of friction was much lower compared with that of sand-rubber contacts and also the slip displacement was significantly shifted for the composite interfaces to larger values compared with that of the pure sand. The micro-slip displacement (after [70]), denoted as d_s, is defined as the threshold shearing displacement where a steady-state sliding is reached (or alternatively, the tangential stiffness reaches zero) so that the interface enters the fully plastic regime of behavior.

For pure LBS contacts, for the set of five experiments performed in the study on different pairs of grains, the average coefficient of friction (μ) was equal to 0.19, while for pure CDV contacts, based again on a set of five different specimens, the average (μ) was found to be equal to 0.43. Despite some scatter in the data, these values (range and average values) are within the reported (μ) by [66] for pure LBS and by [68] for weathered volcanic granules. The experiments on pure rubber specimens showed very high values of (μ), ranging from 0.79 to 0.92 (Table 2) and similarly, very high friction was found for the composite interfaces of LBS-rubber and CDV-rubber. For each class of composite interfaces, the coefficient of friction had a significant scatter, with values ranging from 0.3 to 1.5 and an average (μ) of, approximately, 0.9, while for pure rubber interfaces the values agreed well with reported data on industrial rubber

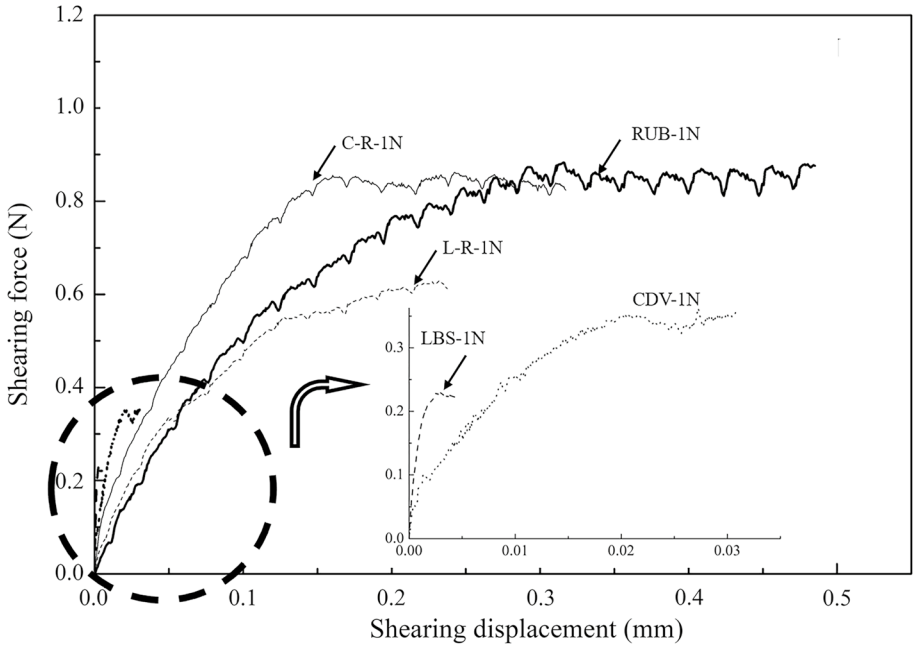

Fig. 3 Representative shearing (tangential) force – displacement curves based on the experiments

Table 2 Monotonic shearing tests on LBS, CDV and rubber interfaces (rigid-rigid and soft–soft contacts)

Material	Shearing rate (mm/h)	F_N (N)	μ	K_{T0} (N/mm)	d_s (μm)
LBS-LBS	0.1	1	0.18	236	3
	0.1	1	0.22	288	2.5
	0.1	1	0.15	200	2
	0.1	1	0.27	127	7
	0.1	1	0.11	150	3
CDV-CDV	0.1	1	0.38	57	25
	0.1	1	0.40	48	25
	0.1	1	0.64	77	35
	0.1	1	0.35	125	20
	0.1	1	0.39	77	30
Rub-Rub	0.2	1	0.79	4	300
	0.2	1	0.81	6	310
	0.2	1	0.92	4	600

tested at room temperature [71–74]. Considering the scatter in the data, probabilistic-based analyses could be implemented in future studies in modeling the behavior of composite interfaces; this type of analysis could be particularly useful in direct implementation of input parameters in DEM simulations of granular and composite materials.

It was observed that the increase in normal load from 1 to 2 N, resulted in slightly decreased values of friction (particularly comparing the average values of μ between 1 and 2 N of normal load). Despite the scatter, the negative relationship between normal load and coefficient of friction shows consistency with the pioneering work by Schallamach [75], which study explained the load dependency of friction on the variation of the true contact area. For pure sand grain contacts, even though most studies have not shown any relationship between friction and normal load, the study by Sandeep and Senetakis [76] showed a slight decrease of friction (μ) as the normal load increases. For composite interfaces however, recent studies published in the literature show a dependency of μ on the applied normal load; this was reported for both composite interfaces of sand grain sliding on softer FRP (fiber-reinforced polymer) interface by He t al. [77] and proppant (natural particle) sliding on softer shale rock by He and Senetakis [78] and He et al. [79]. The dependency of the interparticle friction on the magnitude of normal load is desirable to be considered in DEM simulations (similar to the study by [19]), provided that a complete characterization of the normal load-dependency of interparticle friction at the grain-scale is implemented based on experimental investigations; this can be a promising area of research in future studies.

Compared with the friction of the sand grain contacts (LBS-LBS, CDV-CDV), two mechanisms contribute to the higher interface friction for rubber and composite interfaces (after [73]): (1) molecular adhesion (adhesive friction) for very smooth surfaces and (2) energy losses in the presence of ploughing mechanism for rough and rough-smooth contacts (sliding friction). The study by Pinnington [80] further supported that the sliding friction becomes the dominant mechanism only when the surface wavelength (expressing the surface topology at the small scale) is smaller than the rubber molecules. Given that LBS and CDV are two sands of extremely different morphological characteristics and properties (though both materials are "rough" in a contact

Table 3 Monotonic shearing tests on sand-rubber (soft-rigid) contacts and associate model parameters

Test Number	L-R-1 N			L-R-2 N			C-R-1 N			C-R-2 N		
	μ	K_{T0} (N/mm)	d_s (μm)	μ	K_{T0} (N/mm)	d_s (μm)	μ	K_{T0} (N/mm)	d_s (μm)	μ	K_{T0} (N/mm)	d_s (μm)
1	1.03	20.19	310	1.25	43	550	0.86	27.54	240	0.81	19.5	490
2	0.94	32.42	240	0.95	30.5	480	0.97	28.92	200	0.91	38.67	430
3	0.92	44.64	220	0.63	25.59	200	1.13	21.17	200	1.25	44.42	540
4	0.81	32.76	270	1.20	13.58	570	0.34	18.99	140	0.95	20.18	360
5	1.16	34.48	400	0.94	18.00	490	1.50	26.72	420	0.88	22.16	350
6	0.91	15.78	300	0.9	28.16	405	0.97	22.48	220	0.98	24.3	350
7	1.39	35.74	460	0.62	19.51	320	1.05	39.32	300	0.75	21.82	270
8	0.98	31.94	310	0.98	46.07	370	0.99	19.08	300	0.71	26.48	300
9	0.98	21.52	260	0.76	51.99	360	1.27	24.64	350	0.58	37.04	190
10	1.31	22.26	370	0.76	35.68	245	0.95	23.21	300	0.88	12.27	450
11	0.99	17.91	200	0.86	36.16	210	0.79	24.64	310	0.79	51.01	330
12	1.08	24.64	360	0.85	42.15	370	0.79	12.60	120	0.99	20.10	520
13	0.93	23.88	360	0.59	14.40	310	0.35	24.21	160	0.62	15.2	240
14	0.62	12.60	200	0.92	17.55	400	0.76	15.14	170	1.25	14.05	530
15	0.87	16.76	130	1.03	21.86	430	0.61	26.13	180	0.95	21.84	490
Test-Number	L-R-1 N			L-R-2 N			C-R-1 N			C-R-2 N		
	μ	K_{T0} (N/mm)	d_s (μm)	μ	K_{T0} (N/mm)	d_s (μm)	μ	K_{T0} (N/mm)	d_s (μm)	μ	K_{T0} (N/mm)	d_s (μm)
16	0.71	29.13	210	0.82	33.24	355	1.19	17.61	400	0.48	46.95	110
17	0.55	25.21	170	1.21	43.91	600	1.00	23.79	295	0.43	29.34	160
18	0.73	19.94	230	0.70	45.66	400	0.90	14.4	250	0.86	31.39	410
19	0.84	22.03	260	0.97	30.02	455	1.05	29.12	300	0.75	32.22	320
20	0.93	4.93	310	0.90	27.44	410	0.80	27.36	230	0.7	32.92	480

Table 4 Summary of interparticle friction, tangential stiffness and micro-slip displacement values on soft-rigid interfaces

	L-R-1 N			L-R-2 N			C-R-1 N			C-R-2 N		
	μ	K_{T0} (N/mm)	d_s (μm)	μ	K_{T0} (N/mm)	d_s (μm)	μ	K_{T0} (N/mm)	d_s (μm)	μ	K_{T0} (N/mm)	d_s (μm)
MV	0.93	28.76	270	0.89	31.22	396	0.91	25.96	247	0.83	28.09	366
StD	0.22	10.60	93	0.19	11.62	113	0.28	7.10	84	0.22	11.09	128
CoV	0.23	0.37	0.34	0.22	0.37	0.28	0.31	0.27	0.34	0.26	0.39	0.35

mechanics context), the very similar friction values between LBS-rubber and CDV-rubber imply that the magnitude of surface roughness and other characteristics, which may contribute to the differences between the two sands, are very minor contributing mechanisms in the frictional behavior of the composite interfaces, and that rubber, which is a very soft material with viscous behavior controls the friction. It is noted that Tian et al. [81] quantified the surface roughness of rubber particles and reported an average (RMS) value of approximately 2 microns, which is about 2 times greater than that of the CDV particles and 8 times greater than that of LBS. Despite some influence of the sand grain type, the study by [81] also reported a dominance of the rubber in the normal contact response of sand grain-rubber interfaces subjected to cyclic loading, with an approximate reduction of the normal contact stiffness of one to two orders of magnitude from the pure sand grain contacts to sand grain-rubber composite interfaces (note that the study by [81] investigated a broad range of sand particles, from LBS, to weathered granitic particles as well as grains from basaltic crushed rock). In the shearing direction (results of the present study), it would be expected that the asperities of the LBS sand grains penetrate the much softer surface of the rubber, while for CDV-rubber, even though some penetration might contribute to the frictional mechanisms, the interface is expected to be influenced by the heavy coating of microparticles on the surfaces of the weathered grains; despite these potentially different mechanisms, on a "bulk" scale of grain-over-rubber interface, the properties of the rubber overwhelmingly control the interface response, which is also supported by the

subsequent discussion on the tangential force–displacement relationship, contact stiffness and microslip displacement.

3.2 Microslip displacement and tangential stiffness

Pure rubber interfaces displayed a micro-slip displacement of around 250–300 μm, which is, on average, one order of magnitude greater than that of pure CDV interfaces. Sandeep and Senetakis [67] reported a strong dependency of the micro-slip displacement, which controls the constitutive behavior of interfaces, on material hardness and Young's modulus (as well as surface roughness). Between LBS and CDV, LBS grains are harder (i.e. of greater micro-hardness values) and also of much greater elastic modulus (i.e. Young's modulus and shear modulus) so that the micro-slip displacement found from the experiments on LBS-LBS interfaces is almost one order of magnitude smaller than that of CDV-CDV interfaces. However, for LBS-rubber and CDV-rubber, the slip displacement, the coefficient of friction, and overall, their interface constitutive behavior, are heavily influenced by the rubber (which rubber has extremely low Young's modulus compared with that of geological materials) so that, as also shown in the data of Tables 2 and 3 and the bar graphs in Fig. 4, LBS-rubber and CDV-rubber specimens displayed very similar behavior which was almost independent on the type of sand grains, i.e., the rubber component has a dominant influence on the frictional response of the composite interfaces.

An important parameter in the characterization of the constitutive behavior of interfaces is the tangential stiffness. Despite the scatter in the data for the pure sand grain contacts (Table 2), it is observed that LBS specimens have much

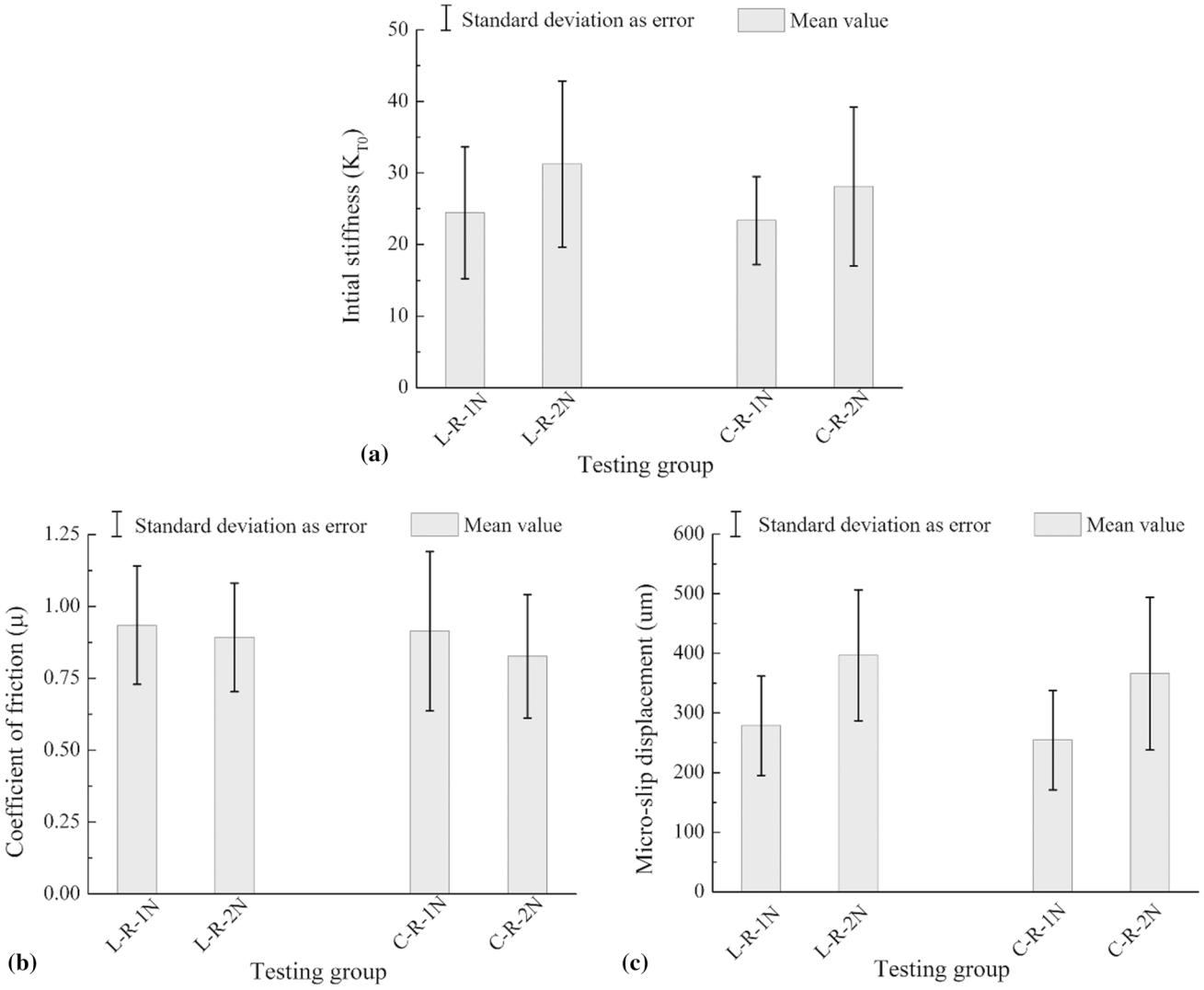

Fig. 4 Standard deviation and mean values of the different contact parameters evaluated experimentally **a** initial stiffness, **b** coefficient of friction and **c** micro-slip displacement

greater values of initial tangential stiffness, K_{T0} (defined at the smallest possible resolvable displacements), almost three times higher on average, compared with that of CDV interfaces. These values, for both LBS and CDV specimens fall within the range of data reported by [62, 69, 76] for quartz and weathered volcanic sand grain contacts. However, the data suggested extremely low K_{T0} values for pure rubber interfaces, which are about one order of magnitude smaller than that of CDV. For composite interfaces, the data in Table 3 and Fig. 4 would suggest that the K_{T0} values are much lower compared with that of pure sand grains. K_{T0} values slightly increased by approximately 8–10% (from 28.8 to 31.2 N/mm for LBS and from 26.0 to 28.1 N/mm for CDV), when the applied normal load increased from 1 to 2 N. The relatively similar values of K_{T0} for both types of sands compared with that of sand-rubber contacts also suggest that the rubber overwhelmingly controls the behavior of the composite interfaces.

3.3 Discussion on the observed frictional behavior of composite interfaces based on Mindlin theory

While the (μ) values of the composite interfaces are found to be very similar with that of pure rubber, K_{T0} values are somewhat greater for the composite interfaces compared with that of pure rubber. The composite shear modulus of the sand-rubber interface would be dominated by the modulus of the rubber itself, as rubber has substantially lower stiffness compared with that of the natural sand grains.

Based on Mindlin theory [82], the relative tangential displacement in the non-slip condition (at the beginning of the shearing) is composed of the elastic deformation of the two contacted bodies, i.e., sand and rubber, as illustrated in Fig. 5.

In Fig. 5, points S_0 and R_0, are coincident points at sand and rubber surfaces before the application of the tangential force. The initial relative displacement (δd_0), and the deformation of sand and rubber (δS and δR) at the incipient stage of sliding evolve in such a way that the two coincident points are displaced at their new locations S_1 and R_1 under the action of a tangential force F_{T0}. Assuming that the contact area follows Hertz theory [83], the relative deformation between S_0 and R_0 equals to the summation of the elastic shear deformation at the two points:

$$\delta d_0 = \delta S - \delta R = \frac{F_{T0}}{8\alpha}\left(\frac{2-v_r}{G_r} + \frac{2-v_s}{G_s}\right) \tag{1}$$

In Eq. (1), α is the Hertzian contact area ($\alpha = \left(\frac{3RF_N}{4E^*}\right)^{\frac{1}{3}}$, where $\frac{1}{E^*} = \frac{1-v_l^2}{E_l} + \frac{1-v_u^2}{E_u}$). R and F_N are the equivalent contact radius and applied normal force, respectively. E_r,v_r,G_r and E_s,v_s,G_s represent the Young's modulus, Poisson's ratio and shear modulus of rubber and sand (subscript "r" for the rubber and subscript "s" for the sand). Given that both δd_0 and F_{T0} increase from zero, the initial stiffness K_{T0}, yields as the equation of Mindlin-Deresiewicz model [84]:

$$K_{T0} = \frac{F_{T0}}{\delta d_0} = 8\left(\frac{3RF_N}{4E^*}\right)^{\frac{1}{3}} G^* \tag{2}$$

In Eq. (2), $G^* = \left(\left(\frac{2-v_s}{G_s} + \frac{2-v_r}{G_r}\right)\right)^{-1}$.

Compared with the tangential loading of the sand-rubber composite interface, the rubber-rubber contact is expected

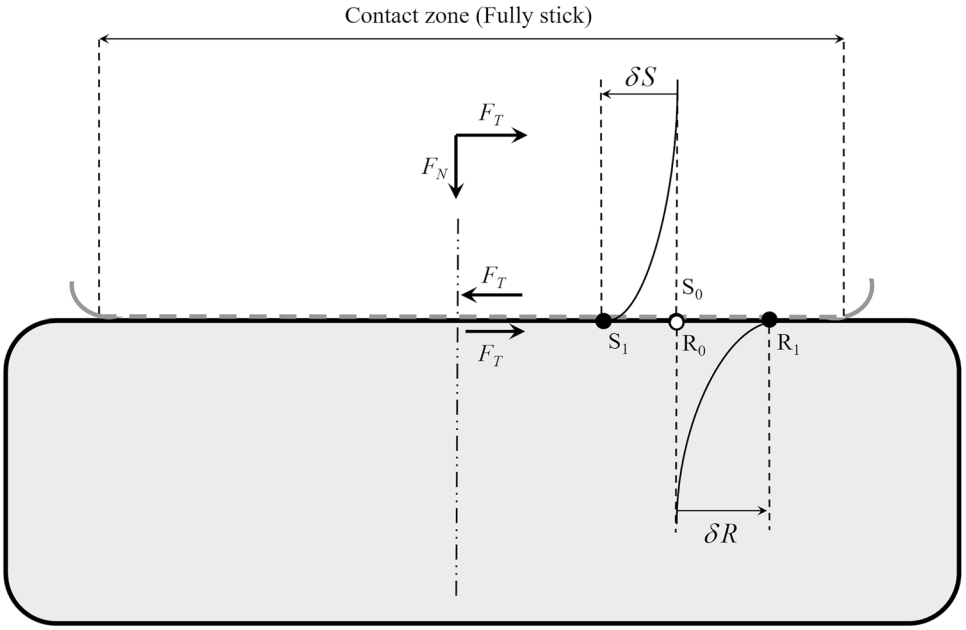

Fig. 5 Schematic illustration of the relative displacements at the incipient stage of inter-particle shearing for soft-rigid interface

to have (i) smaller in magnitude equivalent shear modulus G^*, and (ii) larger contact area $(\frac{3RF_N}{4E^*})^{\frac{1}{3}}$ because of their lower elastic modulus. Suppose that G^* is related with E^* in the same manner shear and Young's moduli are connected through elasticity theory (i.e., $E = \frac{G}{2(1+\nu)}$); in this case the initial tangential stiffness can be expressed as:

$$K_{T0} = C(G^*)^{\frac{2}{3}} \tag{3}$$

where C is a constant which is independent on the contact type (i.e., rubber-rubber or sand-rubber) and it is only determined by the contact radius R and the normal force F_N. Based on Eq. (3), the decrease in G^* will lead in a decrease of stiffness K_{T0}. It may therefore be implied, on a qualitative standpoint, that K_{T0} is always expected to be lower for rubber-rubber compared with sand-rubber contacts.

3.4 Statistical data analysis: correlation between friction and slip displacement and linkage between microscopic observations with reported macroscopic test results

Representative curves of LBS-rubber and CDV-rubber with illustration of the microslip displacement for each case, are given in Fig. 6.

Despite the scatter in the data, it is observed that, in general, curves which display higher values of tangential (or shearing) force also display greater values of microslip displacement, so that this may imply that there is a possibility to provide a correlation between tangential force (or friction) and the slip displacement threshold.

For LBS-rubber and CDV-rubber, an attempt is made to provide different correlations of (i) initial stiffness, (ii) coefficient of friction and (iii) micro-slip displacement (d_s). To illustrate the potential inter-variable dependency, statistical characteristics of these three parameters are further compared in Fig. 7 for LBS-rubber and in Fig. 8 for CDV-rubber. Subfigures in diagonal positions display the

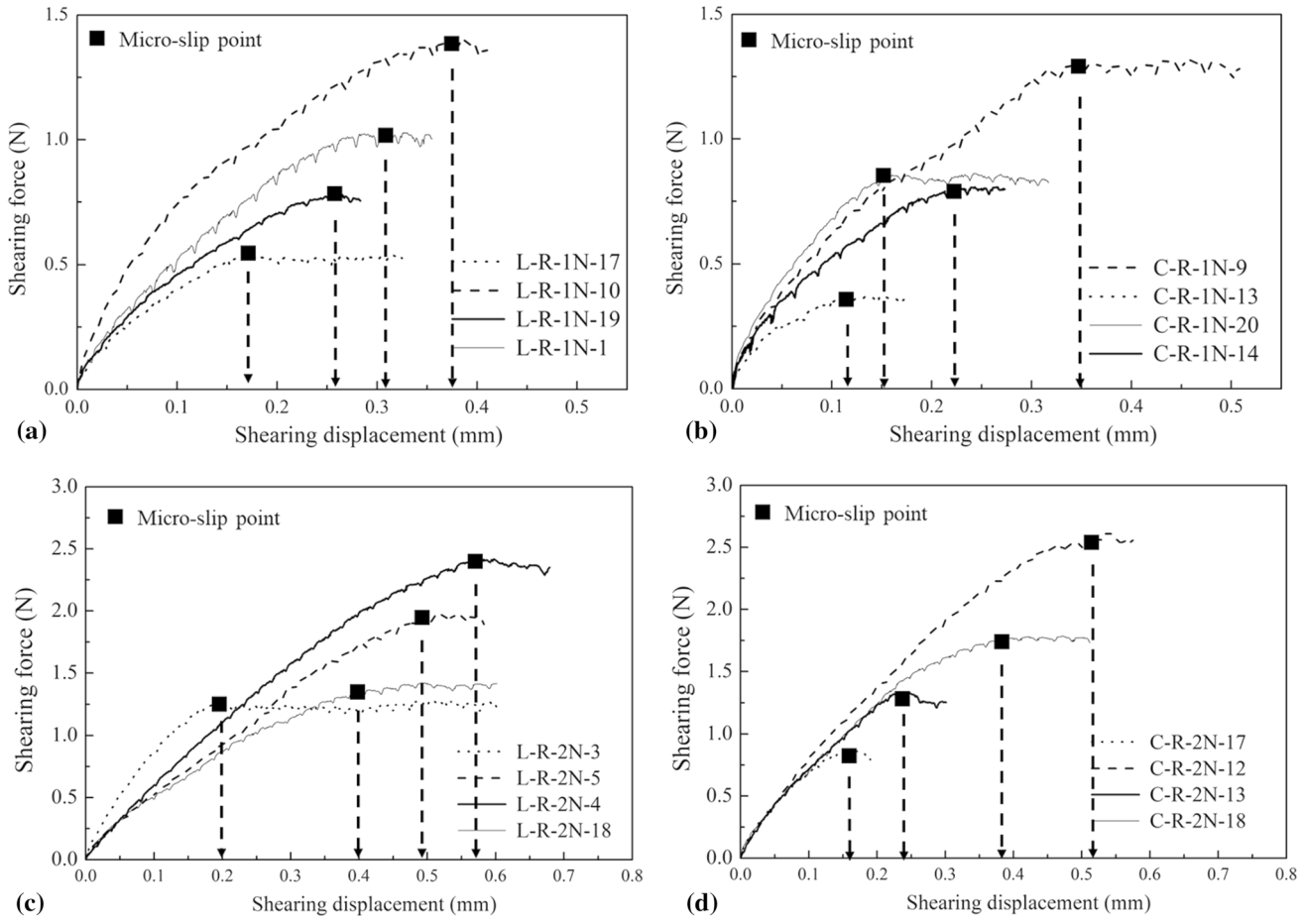

Fig. 6 Experimental shearing force—displacement curves of soft-rigid contacts under different normal loads and associated micro-slip displacements **a** LBS-rubber-1 N **b** CDV-Rubber-1 N **c** LBS-Rubber-2 N **d** CDV-Rubber-1 N

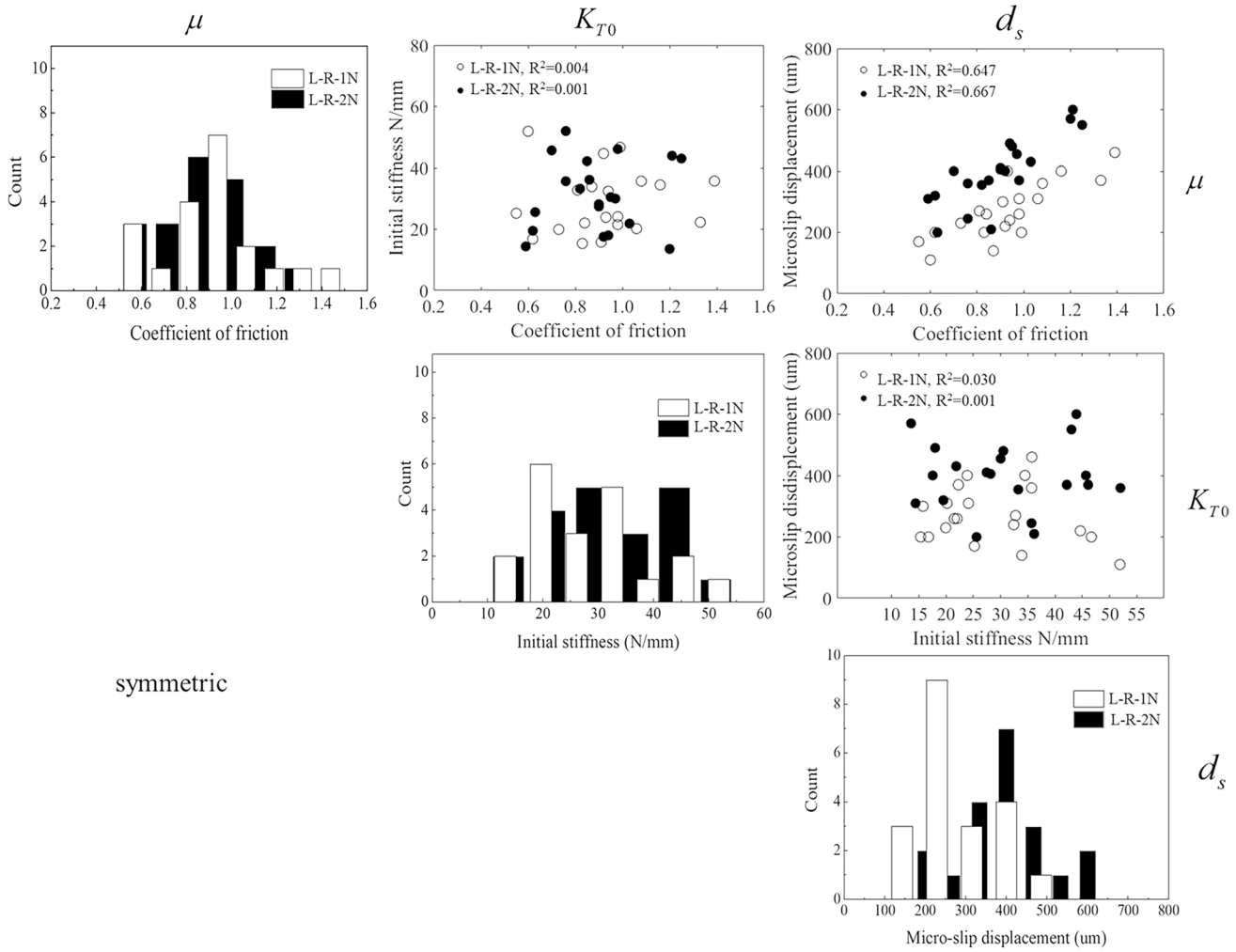

Fig. 7 Relative frequency of contact parameters and associated scatter plots between different variables of LBS-rubber interfaces

histograms of each variable, while the rest show the correlation between elements in row and column.

It is seen in the histograms that some non-uniform distributions can be identified, which spread in a wide range. However, the exact distribution type may not be of major interest to be further analyzed in the present study, but it is rather intended to explore possible correlations between friction, stiffness and slip displacement. For the non-diagonal subfigures, the low R^2 (coefficient of determination) for K_{T0}—μ and K_{T0}–d_s relationships suggest that the initial tangential stiffness does not have a direct correlation with the interface friction or the microslip displacement. However, a clear correlation, despite the scatter, can be observed between friction and microslip displacement (R^2 >0.6) for all the different classes of interfaces. Sandeep and Senetakis [67] verified with experiments that the microslip displacement of pure LBS is inversely proportional to the product of shear modulus, contact area and square root of material hardness, and it increases with the increase of the coefficient of friction, as described by Eq. (4):

$$d_s = \frac{9(2-\nu)\mu F_N}{16G\alpha\sqrt{H_N}} \tag{4}$$

where H_N denotes the hardness of the material while the other terms follow the definition in the previous discussion.

In this study, the contacts over rubber exhibit much softer hardness and shear modulus and larger friction so that Eq. (4), which was derived from pure sand grain contacts, can also explain, qualitatively, the occurrence of the larger micro-slip displacements for the composite interfaces. In particular, the positive correlation between μ and d_s in Eq. (4) agrees with the experimental observations in Figs. 7 and 8.

The results on sand-rubber interfaces highlight the significant shift of the non-linear elastic–plastic regime of behavior compared with that of pure sand grain contacts,

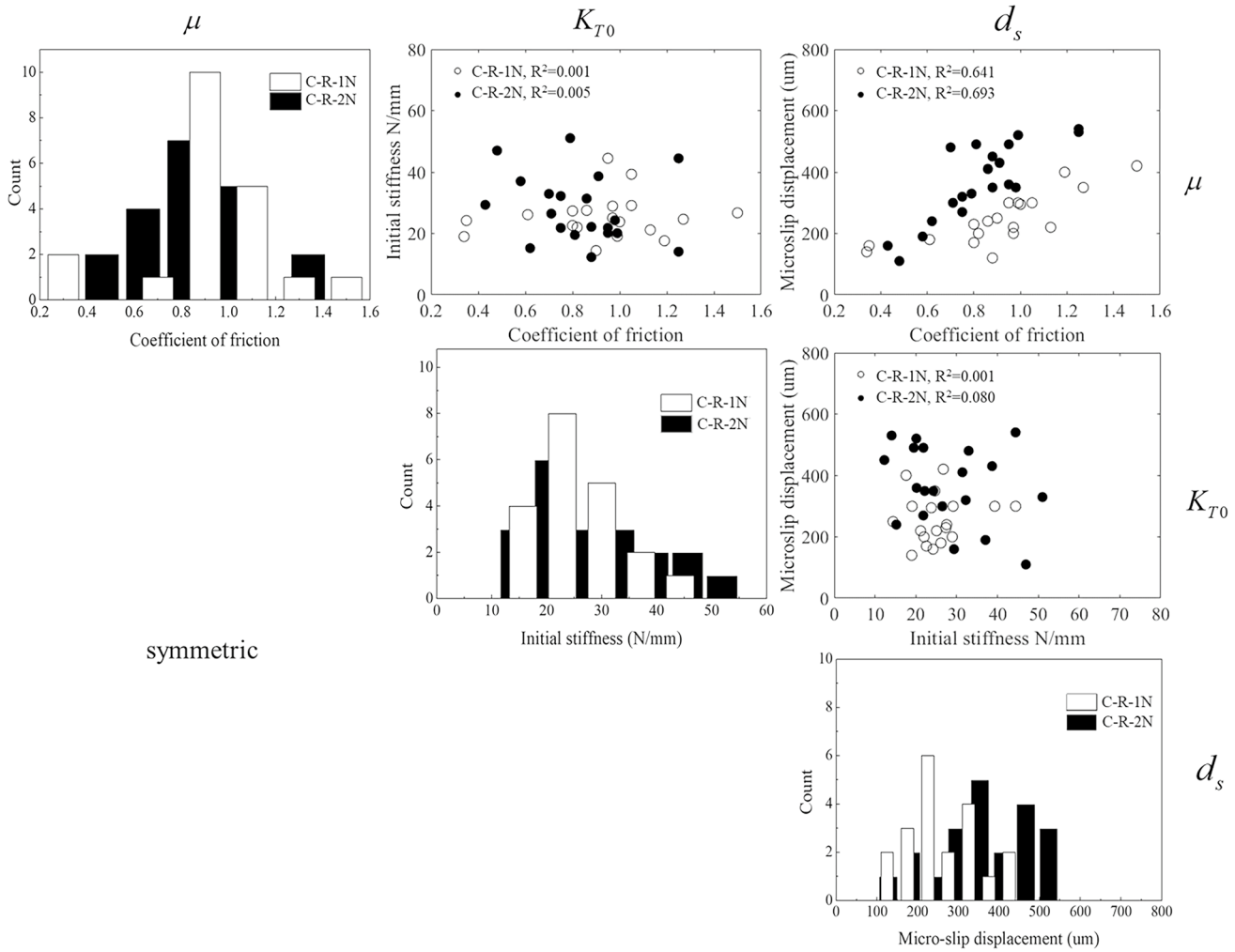

Fig. 8 Relative frequency of contact parameters and associated scatter plots between different variables of CDV-rubber interfaces

which, in turn, may provide micromechanical-based explanations on the observed influence of rubber inclusion, even at small percentages, on the increase of the non-linear range of behavior as reported in macroscopic experiments by [28]. Despite the increase in compressibility when rubber is added in soil mixtures, the very high interparticle friction at the contacts of sand-rubber (and rubber-rubber) can also provide some qualitative explanations of the positive contribution of sand-rubber contacts in the load carrying mechanisms of sand-rubber mixtures as reported in the DEM studies by [20, 21]. Previous studies have reported satisfactory strength characteristics of sand-rubber mixtures, both in terms of peak strength and critical state behavior [3, 9, 11, 16]; even though attempts have been made to explain this contribution of rubber on the mobilization of its tensile resistance, the results in the present study suggest that the increase in interparticle friction may have a dominant contribution, as also the study by Li et al. [15] would suggest.

However it is also acknowledged, regarding a granular assembly which consists of rigid and soft grains, that the contact loading state can be very complex in a way that both the magnitude and direction of the normal and tangential forces vary simultaneously. The observed interactions between soft and rigid phases including twisting, squeezing and separation [85] could be more complex considering other effects, such as rubber fraction, size ratio and rubber shape [86, 87]. Reproducing the realistic interaction in experiments is a complex and challenging task; hence the advancement of numerical tools such as algorithms given by Mollon [88] or Nezamabadi et al. [89] can be very promising. However, the power of numerical tools can be further enhanced with the benchmark properties at the composite interfaces derived from the "simplified loading state".

3.5 Application of the Mindlin-Deresiewicz (M-D) model accounting for experimental stiffness but exclusing the self-deformation of rubber

Mindlin-Deresiewicz model referred to as M-D model [84], considers a case of identical elastic spheres in contact and describes the tangential contact stiffness reduction with increasing tangential force. This non-linear model has been extensively reported in discrete-based modeling of granular materials, and is expressed as:

$$K_t^n = K_{T0}(1 - \frac{F_T^{n-1}}{\mu F_N})^{\frac{1}{3}} \tag{5}$$

$$K_{T0} = \frac{8aG^*}{2-v} \tag{6}$$

$$F_T^{n+1} = F_T^n + K_t^{n+1}\Delta d_t \tag{7}$$

In Eq. (5), K_t^n and F_T^n correspond to the tangential stiffness and tangential force, respectively, during shearing at the nth displacement increment. μ and F_N denote the coefficient of friction and the applied normal load, respectively. K_{T0} is the initial tangential stiffness, whose theoretical value is displayed in Eq. (6). Note that each notation in Eq. (6) follows the definition in Eqs. (1)-(2).

The theoretical tangential stiffness K_{T0} in the M-D model is calculated based on the contact radius and elastic modulus of the materials. Recent works [58, 90–93] would suggest that implementing, directly, the original M-D model, to fit the experimental tangential load–displacement curves is highly ineffective and that modifications of the model, or alternatively, implementation directly into the M-D expression of the measured tangential stiffness is necessary to provide better matching between experiment and model prediction. Hence in this study, K_{T0} implemented into the M-D model refers to the experimental stiffness (i.e. stiffness listed in Table 3) for each attempt of fitting unless otherwise specified. Figure 9 displays representative attempts to fit the M-D model to the experimental curves for CDV-rubber and LBS-rubber contacts under normal loads of 1 N in Fig. 9a and 2 N in Fig. 9b. These data show that, even though experimental tangential stiffness is used, there is poor matching between M-D model and laboratory-based results.

In specific, the M-D model highly underestimates the microslip displacements, thus leading to a much faster reduction of stiffness and early entrance into the fully plastic regime of behavior. It is noted, as also mentioned in the studies by [67, 90], that it is not only the initial tangential stiffness, but, perhaps, also the rate of stiffness reduction that should be taken into account for realistic implementation of the M-D model in capturing the behavior of real soil grain

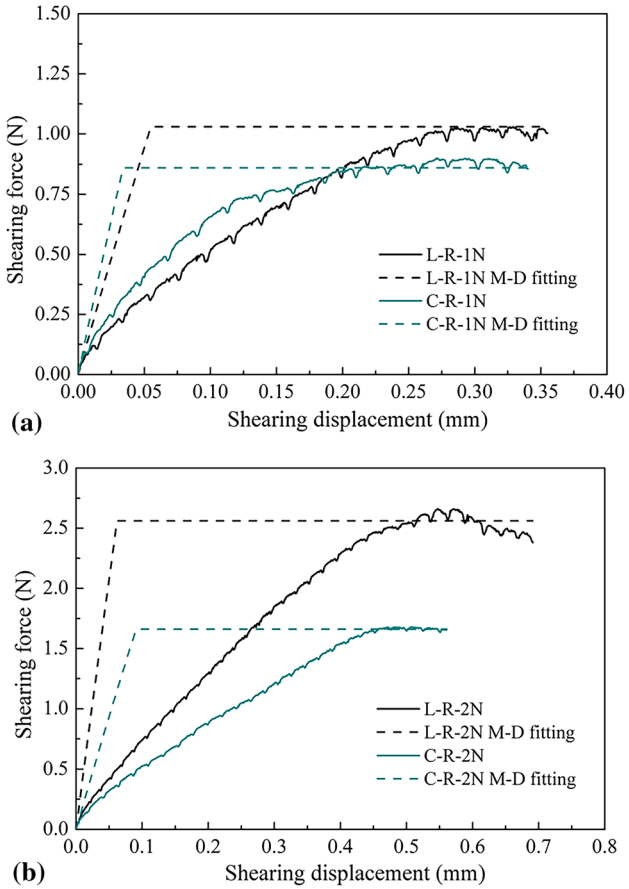

Fig. 9 Implementation of Mindlin-Deresiewicz model in the fitting process of experimental curves considering experimental initial tangential stiffness but without consideration of the self-deformations of the rubber

contacts. In their grain-scale study on interfaces of pumice, He and Senetakis [91] proposed an alternative approach in dealing with this problem by correlating interparticle friction with the power-value of the M-D model, which, indirectly, takes into account the micro-slip displacement. For sand-rubber interfaces, the mismatch between M-D model and experimental curves is overwhelming, even though experimental initial stiffness values are used.

The original M-D model established the non-linear relationship between shearing and the accumulation of relative displacement of the interfaces, as expressed in Eq. (1). The accurate measurement of such displacement is too subtle for any micro-mechanical experiment on sand grains and hence, an approximation was adopted for the shearing problem of rigid sand in such a way that the measured displacement of two grains is considered as the relative displacement of the interfaces, i.e., Δd_t in Eq. (7) denotes the shearing displacement of two grains. However, such an approximation becomes problematic for soft bodies such as rubber, for which the shear force is so large that the self-deformation is no longer negligible. In

other words, the experimental shearing displacement might have, inherently, overestimated the relative displacement of the sand and rubber, because of the higher coefficient of friction as well as the lower shear modulus of the composite interface. Thus, the self-deformation of rubber might have also contributed to the discrepancies between experimental and theoretical curves, indicating that a correction to the measured shearing displacement might be a rational approach to be applied. In this study, an attempt of modifying the existing model is provided by addressing the mismatch of the experimental values.

3.6 Modification of the M-D model: correction taking into account the self-deformation of rubber

It was attempted to split the experimentally measured displacement (d) into the relative displacement (d_r) and the self-deformation displacement, assuming d_r is proportional to the shearing force. Since each shearing displacement value on each curve corresponds to a single shearing force before micro-slip occurs, a function $g(d)$ is postulated, hypothesising that $d_r = g(d)d$ and that g(d) and d follow a linear relationship (i.e., $g(d) = ad + \beta$). For simplicity, the total shearing displacement can be further normalized by the micro-slip displacement d_s, so that $g(d)$ is expressed in Eq. (8).

$$g(d) = \alpha\frac{d}{d_s} + \beta \tag{8}$$

where, the relative displacement, can be defined as: $d_r = g(d)d = \alpha\frac{d^2}{d_s} + d\beta$.

M-D model (Eqs. (5)-(7)) describes the relationship between incremental shearing displacement Δd and tangential stiffness K_T. Alternatively, the M-D model can also be expressed in terms of the total displacement and the shearing force [94], as displayed in Eq. (9):

$$F_T = \mu F_N\left[1 - (1 - \frac{2K_{T0}d}{3\mu F_N})^{\frac{3}{2}}\right] \tag{9}$$

Each term in Eq. (9) keeps the same physical meaning as the preceding discussion. In particular, Eq. (9) can be revised for interparticle shearing between sand and rubber, considering that only relative displacement contributes to the interface shearing force:

$$F_T = \mu F_N\left[1 - (1 - \frac{2K_{T0}[g(d)d]}{3\mu F_N})^{\frac{3}{2}}\right] \tag{10}$$

which is equivalent to Eq. (11), as:

$$1 - (1 - \frac{F_T}{\mu F_N})^{\frac{2}{3}} = \frac{2K_{T0}[g(d)d]}{3\mu F_N} \tag{11}$$

Differentiating both sides of Eq. (11) with respect to the shearing force (i.e. $\partial d/\partial F_T$) yields the following expression:

$$\frac{1}{K_{T0}(g(d) + \frac{\partial g(d)}{\partial d}d)}(1 - \frac{F_T}{\mu F_N})^{-\frac{1}{3}} = \frac{\partial d}{\partial F_T} = \frac{1}{K_T} \tag{12}$$

Substituting Eq. (8) into Eq. (12), the tangential stiffness after correction can be expressed as:

$$K_t = (2\alpha\frac{d}{d_s} + \beta)K_{T0}(1 - \frac{F_T^{n-1}}{\mu F_N})^{\frac{1}{3}} \tag{13}$$

where α and β in Eq. (13) denote two material constants for an individual contact and they should satisfy the following relationship to ensure $g(d)$ ranges from 0 to 1:

$$\begin{cases} 0 \le \beta \le 1 \\ -\frac{\beta}{2} \le \alpha \le \frac{1-\beta}{2} \end{cases} \tag{14}$$

Similar to the fitting process discussed previously, the modified M-D model based on Eq. (13) was applied to the same set of experimental curves discussed in Fig. 9. Each attempt in the modeling process uses different combination of α and β (with 0.025 spacing) and a Matlab code was developed for this iteration process so that to implement a least square error approach in the final fitting. A comparison between theoretical and experimental curves is shown in Fig. 10 based on the aforementioned modifications of the M-D model. In this case, the results show a more satisfactory fitting, as the implementation of realistic micro-slip displacement seems to control the effectiveness of the M-D model in representing the behavior of the composite contacts. K_{T0} in this study was calculated as a secant stiffness at 2 μm of shearing displacement, i.e., initial tangential stiffness approximates a tangent value, but in reality it is computed taking into account a set of points averaging the stiffness at the smallest resolvable displacements. Based on this, self-deformation of rubber is effectively included. Such an approximation slightly underestimates the real K_{T0} (which should correspond directly to the tangent value) after the correction is applied, but, based on the methodology and experimental procedure, it would not be reliable to pick up the very first point (of recorded force and displacement) to derive stiffness. Despite that, the modification of the M-D model and the corresponding model fitting highlight the importance in taking into account "self-deformations" in analyzing the micromechanical response of sand-rubber composite interfaces.

It should be noted that the self-deformation of rubber was considered in an empirical way, rather than based on a rigorous constitutive calculation. In future works, the deformation of rubber might be considered more explicitly with the assistance of advanced experimental measurements and the use of

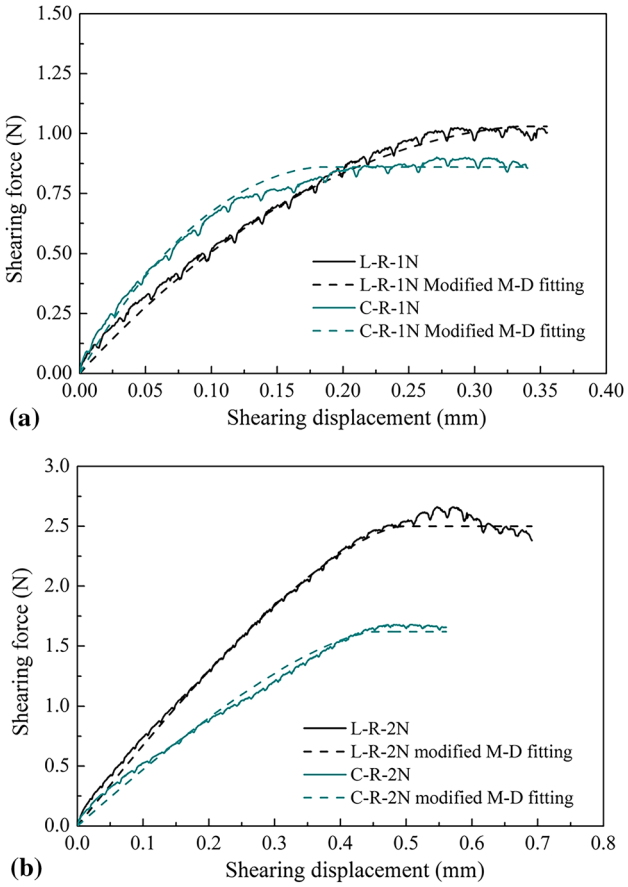

Fig. 10 Implementation of Mindlin-Deresiewicz model in the fitting process of experimental curves considering experimental initial tangential stiffness with consideration of the self-deformations of the rubber

state-of-art numerical tools, such as a meshfree algorithm as proposed by Mollon [86]. Hence the attempt in the present study only intends to provide a rational concept to deal with the significant mismatch between experiments and theory rather than to give a standard solution for the contact problem of deformable interfaces (or, more precisely grain-deformable block in the present study). The greatly improved fitting, based on these considerations, imply that the concept of displacement correction is feasible, at least to some extent, to match the inter-particle constitutive response in the modeling process of granulated rubber in DEM, where the simulation would be very difficult by considering rubber deformations using rigid grains [13]. This approach may have further implications to other types of problems, for example involving grain-flexible barrier interactions in granular flows or the analysis of other geosynthetics and composite systems.

4 Conclusions

Based on the micromechanical test results on sand-rubber interfaces and the subsequent analysis using contact mechanics models, the major conclusions from the study are summarized as:

1. Rubber dominates the contact behavior of sand-rubber interfaces in the tangential direction. On average, the test results showed higher interparticle friction, lower tangential (shearing) stiffness, and much larger micro-slip displacements for sand-rubber contacts compared with that of sand-sand contacts.
2. The tribological parameters examined in the study for sand-rubber composite interfaces, including friction, contact stiffness and micro-slip displacement, were found to display scatter in their values, compared with those for pure sand grain contacts. This gives some promising directions in future works implementing probablistic-based approaches in modeling the contact problem of sand-rubber interfaces. However, it is needed to be noticed that the results and major observed trends were very clear (i.e., the way friction, stiffness or micro-slip displacement are affected by rubber) and they were found to be almost independent on the sand type, which also implies an overwhelming influence of the rubber surface. A positive correlation was found between the coefficient of friction and the micro-slip displacement indicating a useful guideline in the implementation of realistic input parameters in discrete-based numerical studies of granular composite materials.
3. The application of the Mindlin-Deresiewicz (M-D) model to fit the experimental data showed very poor prediction (or matching) with what the micromechanical-based laboratory test results showed. This was ascribed, predominantly, to the significant underestimation of the micro-slip displacement of the sand-rubber contacts from the M-D model. It was hypothesized that the self-deformation of the soft rubber under the action of shearing forces leads to these discrepancies between theory and measurement. Based on this, a "correction" process was introduced into the M-D model (i.e., a correction factor), which process was based on some simple assumptions including the contribution of rubber deformation. This led to a modification of the M-D model which then provided very satisfactory modeling of the experimental tangential force–displacement curves of the composite interfaces. The successful application of the correction factor into the M-D model may also bring some new insights and suggestions in the process

of reconstructing contact mechanics models which may be more applicable for real soil grain interfaces or soil grain-composite systems such as sand-rubber.

Acknowledgements The work described in this paper was fully supported by grants from the Research Grants Council of the Hong Kong Special Administrative Region, China, project no. "CityU 11210419" and project no. "CityU 11214218" and the SRG-Fd grant by City University of Hong Kong, project no. "7005545".

Declarations

Conflict of interest The authors declare no conflict of interest from the present study. This work contains original material as a result of purely academic study without any kind of private funding or other conflict of interest.

References

1. Foose, G.J., Benson, C.H., Bosscher, P.J.: Sand reinforced with shredded waste tires. J Geotech. Eng. **122**(9), 760–767 (1996)
2. Edil, TB.: A review of mechanical and chemical properties of shredded tires and soil mixtures. geotechnical special publication,No. 127, ASCE; 1–21 (2004)
3. Youwai, S., Bergado, D.T.: Strength and deformation characteristics of shredded rubber tire sand mixtures. Can. Geotech. J. **40**(2), 254–264 (2003)
4. Zornberg, J.G., Cabral, A.R., Viratjandr, C.: Behaviour of tire shred sand mixtures. Can. Geotech. J. **41**(2), 227–241 (2004)
5. Lee, J.S., Dodds, J., Santamarina, J.C.: Behavior of rigid-soft particle mixtures. J. Mater. Civ. Eng. **19**(2), 179–184 (2007)
6. Lee, C., Shin, H., Lee, J.S.: Behavior of sand–rubber particle mixtures: experimental observations and numerical simulations. Int. J. Numer. Methods Eng. **38**(16), 1651–1663 (2014)
7. Kim, H.K., Santamarina, J.C.: Sand–rubber mixtures (large rubber chips). Can. Geotech. J. **45**(10), 1457–1466 (2008)
8. Fu, R., Coop, M.R., Li, X.Q.: Influence of particle type on the mechanics of sand–rubber mixtures. J. Geotech. Geoenviron. **143**(9), 04017059 (2017)
9. Fu, R., Coop, M.R., Li, X.Q.: The mechanics of a compressive sand mixed with tyre rubber. Geotech. Lett. **4**(3), 238–243 (2014)
10. Ehsani, M., Shariatmadari, N., Mirhosseini, S.: Shear modulus and damping ratio of sand-granulated rubber mixtures. J. Central South Univ. **22**(8), 3159–3167 (2015)
11. Mashiri, M., Vinod, J., Sheikh, M.N., Tsang, H.-H.: Shear strength and dilatancy behaviour of sand–tyre chip mixtures. Soils Found **55**(3), 517–528 (2015)
12. Zhou, W., Xu, K., Ma, G., Yang, L., Chang, X.: Effects of particle size ratio on the macro-and microscopic behaviors of binary mixtures at the maximum packing efficiency state. Granular Matter **18**(4), 81 (2016)
13. Platzer, A., Rouhanifar, S., Richard, P., Cazacliu, B., Ibraim, E.: Sand–rubber mixtures undergoing isotropic loading: derivation and experimental probing of a physical model. Granular Matter **20**(4), 81 (2018)
14. Wang, C., Deng, A., Taheri, A.: Three-dimensional discrete element modeling of direct shear test for granular rubber–sand. Comput. Geotech. **97**, 204–216 (2018)
15. Li, W., Kwok, C.Y., Sandeep, C.S., Senetakis, K.: Sand type effect on the behaviour of sand-granulated rubber mixtures: integrated study from micro-to macro-scales. Powder Technol. **342**, 907–916 (2019)
16. Li, W., Kwok, C.Y., Senetakis, K.: Effects of inclusion of granulated rubber tyres on the mechanical behaviour of a compressive sand. Can. Geotech. J. **57**(5), 763–769 (2019)
17. ASTM. Standard practice for use of scrap tires in civil engineering applications. ASTM D6270–98, West Conshohoken, Pa,USA; (2008)
18. ASTM. Testing and specification of recycled materials for sustainable geotechnical construction: J. ASTM Int., Selected Technical Papers STP 1540 (Edil T., Ed.), ASTM, West Conshohochen, Pa, USA; (2012)
19. Valdes, J.R., Evans, T.M.: Sand–rubber mixtures: experiments and numerical simulations. Can. Geotech. J. **45**(4), 588–595 (2008)
20. Lopera Perez, J.C., Kwok, C.Y., Senetakis, K.: Effect of rubber size on the behaviour of sand-rubber mixtures: a numerical investigation. Comput. Geotech. **80**, 199–214 (2016)
21. Lopera Perez, J.C., Kwok, C.Y., Senetakis, K.: Investigation of the micro-mechanics of sand–rubber mixtures at very small strains. Geosynth. Int. **24**(1), 30–44 (2017)
22. Lopera Perez, J.C., Kwok, C.Y., Senetakis, K.: Micromechanical analyses of the effect of rubber size and content on sand-rubber mixtures at the critical state. Geotext. Geomembr. **45**(2), 81–97 (2017)
23. Wu, K., Rémond, K., Abriak, N., Pizette, P., Becquart, F., Liu, S.: Study of the shear behavior of binary granular materials by DEM simulations and experimental triaxial tests. Adv. Powder Technol. **28**(9), 2198–2210 (2017)
24. Asadi, M., Thoeni, K., Mahboubi, A.: An experimental and numerical study on the compressive behavior of sand-rubber particle mixtures. Comput. Geotech. **104**, 185–195 (2018)
25. Nie, Z., Zhu, Y., Zou, J., Gong, J., Liu, S.: DEM study of the microscopic characteristics and internal stability of binary mixtures. Powder Technol. **352**, 314–324 (2019)
26. Zhang, J., Chen, X., Zhang, J., Wang, X.: Microscopic investigation of the packing features of soft-rigid particle mixtures using the discrete element method. Adv. Powder Technol. **31**(7), 2951–2963 (2020)
27. Anastasiadis, A., Senetakis, K., Pitilakis, K.: Small-strain shear modulus and damping ratio of sand-rubber and gravel-rubber mixtures. Geotech. Geol. Eng **30**(2), 363–382 (2012)
28. Senetakis, K., Anastasiadis, A., Pitilakis, K.: Dynamic properties of dry sand/rubber (SRM) and gravel/rubber (GRM) mixtures in a wide range of shearing strain amplitudes. Soil Dyn. Earthq. Eng. **33**(1), 38–53 (2012)
29. Cavarretta, I., Coop, M.R., Osullivan, C.: The influence of particle characteristics on the behavior of coarse grained soils. Geotechnique **60**(6), 413–423 (2010)
30. Hurley, R.C., Andrade, J.E.: Friction in inertial granular flows: competition between dilation and grain-scale dissipation rates. Granular Matter **17**(3), 287–295 (2015)
31. Marzulli, V., Sandeep, C.S., Senetakis, K., Cafaro, F., Pöschel, T.: Scale and water effects on the friction angles of two granular soils with different roughness. Powder Technol. **377**, 813–826 (2021)
32. Thornton, C.: Numerical simulations of deviatoric shear deformation of granular media. Geotechnique **50**(1), 43–53 (2000)
33. Yimsiri, S., Soga, K.: Micromechanics-based stress–strain behaviour of soils at small strains. Geotechnique **50**(5), 559–571 (2000)
34. Barreto, D., O'Sullivan, C.: The influence of inter-particle friction and the intermediate stress ratio on soil response under generalised stress conditions. Granular Matter **14**(4), 505–521 (2012)
35. Yang, Z.X., Yang, J., Wang, L.Z.: On the influence of inter-particle friction and dilatancy in granular materials: a numerical analysis. Granular Matter **14**(3), 433–447 (2012)

36. Sazzad, M.M., Suzuki, K.: Effect of interparticle friction on the cyclic behavior of granular materials using 2D DEM. J. Geotech. Geoenviron. **137**(5), 545–549 (2011)
37. Huang, X., Hanley, K.J., O'Sullivan, C., Kwok, C.Y.: Exploring the influence of interparticle friction on critical state behaviour using DEM. Int. J. Numer. Methods Eng. **38**(12), 1276–1297 (2014)
38. Kawamoto, R., Andò, E., Viggiani, G., Andrade, J.E.: All you need is shape: Predicting shear banding in sand with LSDEM. J. Mech. Phys. Solids **111**, 375–392 (2018)
39. Nadimi, S., Otsubo, M., Fonseca, J., O'Sullivan, C.: Numerical modelling of rough particle contacts subject to normal and tangential loading. Granular Matter (2019). https://doi.org/10.1007/s10035-019-0970-y
40. Mollon, G., Quacquarelli, A., Andò, E., Viggiani, G.: Can friction replace roughness in the numerical simulation of granular materials? Granular Matter **22**(2), 1–16 (2020)
41. Nadimi, S., Ghanbarzadeh, A., Neville, A., Ghadiri, M.: Effect of particle roughness on the bulk deformation using coupled boundary element and discrete element methods. Comput. Part. Mech. **7**, 603–613 (2020)
42. Otsubo, M., O'Sullivan, C.: Experimental and DEM assessment of the stress-dependency of surface roughness effects on shear modulus. Soils Found **58**(3), 602–614 (2018)
43. Guillard, F., Marks, B., Einav, I.: Dynamic X-ray radiography reveals particle size and shape orientation fields during granular flow. Sci. Rep. **7**(1), 8155 (2017)
44. Misra, A.: Effect of asperity damage on shear behavior of single fracture. Eng. Fract. Mech. **69**, 1997–2014 (2002)
45. Misra, A., Marangos, O.: Effect of contact viscosity and roughness on interface and wave propagation. AIP Conf. Proc. **1096**(1), 105 (2009). https://doi.org/10.1063/1.3114071
46. Huang, S., Misra, A.: Micro–Macro-Shear-Displacement behavior of contacting rough solids. Tribol Lett. **51**, 431–436 (2013)
47. Pohrt, R., Popov, V.L.: Normal contact stiffness of elastic solids with fractal rough surfaces. Phys. Rev. Lett. **108**(10), 104301 (2012)
48. Persson, B.N.J.: Relation between interfacial separation and load: a general theory of contact mechanics. Phys. Rev. let. **99**(12), 125502 (2007)
49. Guo, N., Zhao, J.D.: Multiscale insights into classical geomechanics problems. Int. J. Numer. Anal Meth. Geomech. **40**(3), 367–390 (2016)
50. Marks, B., Einav, I.: A heterarchical multiscale model for granular materials with evolving grainsize distribution. Granular Matter **19**(3), 61 (2017). https://doi.org/10.1007/s10035-017-0741-6
51. Hurley, R.C., Hall, S.A., Andrade, J.E., Wright, J.: Quantifying interparticle forces and heterogeneity in 3D granular materials. Phys. Rev. Lett. **117**, 098005 (2016)
52. Guida, G., Einav, I., Marks, B., Casini, F.: Linking micro grainsize polydispersity to macro porosity. Int. J. Solids Struct. **187**, 75–84 (2020)
53. Marks, B., Rognon, P., Einav, I.: Grainsize dynamics of polydisperse granular segregation down inclined planes. J. Fluid Mech. **690**, 499–511 (2012)
54. Cole, D.M., Peters, J.F.: A physically based approach to granular media mechanics: grain-scale experiments, initial results and implications to numerical modeling. Granular Matter **9**(5), 309–321 (2007)
55. Senetakis, K., Coop, M.R.: The development of a new micromechanical inter-particle loading apparatus. Geotech. Test J. **37**(6), 1028–1039 (2014)
56. Hanaor, D.A.H., Gan, Y., Einav, I.: Effects of surface structure deformation on static friction at fractal interfaces. Geotech. Lett. **3**(2), 52–58 (2013)
57. Yang, L., Wang, D., Guo, Y., Liu, S.: Tribological behaviors of quartz sand particles for hydraulic fracturing. Tribol. Int. **102**, 485–496 (2016)
58. Nardelli, V., Coop, M.R., Andrade, J.E., Paccagnella, F.: An experimental investigation of the micromechanics of Eglin sand. Powder Technol **312**, 166–174 (2017)
59. Ren, J., He, H., Senetakis, K.: A Micromechanical-based investigation on the frictional behaviour of artificially bonded analogue sedimentary rock with calcium carbonate. Pure Appl. Geophys. (2021). https://doi.org/10.1007/s00024-021-02875-z
60. He, H., Senetakis, K., Coop, M.R.: An investigation of the effect of shearing velocity on the inter-particle behavior of granular and composite materials with a new micromechanical dynamic testing apparatus. Tribol Int. **134**, 252–263 (2019)
61. Sandeep, C.S., Senetakis, K.: Micromechanical experiments using a new inter-granule loading apparatus for gravel-to-ballast sized materials. Friction **8**(1), 70–82 (2020)
62. Sandeep, C.S., He, H., Senetakis, K.: An experimental micromechanical study of sand grain contacts behavior from different geological environments. Eng. Geol. **246**, 176–186 (2018)
63. Ren, J., Li, S., He, H., Senetakis, K.: The tribological behavior of iron tailing sand grain contacts in dry, water and biopolymer immersed states. Granular Matter **23**(1), 12 (2020). https://doi.org/10.1007/s10035-020-01068-0
64. Sandeep, C.S., Li, S., Senetakis, K.: Scale and surface morphology effects on the micromechanical contact behavior of granular materials. Tribol. Int. **159**, 106929 (2021). https://doi.org/10.1016/j.triboint.2021.106929
65. Tsang, H.H.: Seismic isolation by rubber–soil mixtures for developing countries. Earthq. Eng. Struct. Dyn. **37**(2), 283–303 (2008)
66. Sandeep, C.S., Senetakis, K.: Effect of Young's modulus and surface roughness on the inter-particle friction of granular materials. Materials **11**(2), 217 (2018)
67. Sandeep, C.S., Senetakis, K.: An experimental investigation of the microslip displacement of geological materials. Comput. Geotech. **107**, 55–67 (2019)
68. Sandeep, C.S., Todisco, M.C., Senetakis, K.: Tangential contact behaviour of a weathered volcanic landslide material from Hong Kong. Soils Found **57**(6), 1096–1102 (2017)
69. Sandeep, C.S., Todisco, M., Nardelli, V., Senetakis, K., Coop, M.R., Lourenco, S.: A micromechanical experimental study of highly/completely decomposed tuff granules. Acta Geotech. **13**(6), 1355–1367 (2018)
70. Olsson, E., Larsson, P.L.: On the tangential contact behavior of elastic-plastic spherical contact problems. Wear **319**, 110–117 (2014)
71. Bielsa, J.M., Canales, M., Martínez, F.J.: Application of finite element simulations for data reduction of experimental friction tests on rubber–metal contacts. Tribol Int. **43**(4), 785–795 (2010)
72. Gómez, M.C., Gallardo-Hernandez, E.A., Torres, M.V., Bautista, A.P.: Rubber steel friction in contaminated contacts. Wear **302**(1–2), 1421–1425 (2013)
73. Grosch, K.A.: The relation between the friction and visco-elastic properties of rubber. Pro R Soc Lond A **274**(1356), 21–39 (1963)
74. Hale, J., Lewis, R., Carré, M.J.: Rubber friction and the effect of shape. Tribol Int **141**, 105911 (2020)
75. Schallamach, A.: The load dependence of rubber friction. Proc. Phy. Soc. Sec. B **65**(9), 657 (1952)
76. Sandeep, C.S., Senetakis, K.: Grain-Scale mechanics of quartz sand under normal and tangential loading. Tribol Int **117**, 261–271 (2018)
77. He, H., Chen, W., Yin, Z.Y., Senetakis, K., Yin, J.H.: A micromechanical-based study on the tribological and creep-relaxation behavior of sand-FRP composite interfaces. Compos. Struct. **275**, 114423 (2021). https://doi.org/10.1016/j.compstruct.2021.114423

78. He, H., Senetakis, K.: A micromechanical study of shale rock-proppant composite interface. J. Petrol. Sci. Eng. **184**, 106542 (2020). https://doi.org/10.1016/j.petrol.2019.106542
79. He, H., Luo, L., Senetakis, K.: Effect of normal load and shearing velocity on the interface friction of organic shale – proppant simulant. Tribol. Int. **144**, 106119 (2020). https://doi.org/10.1016/j.triboint.2019.106119.144,106119
80. Pinnington, R.J.: Rubber friction on rough and smooth surfaces. Wear **267**(9–10), 1653–1664 (2009)
81. Tian, Y., Kasyap, S.S., Senetakis, K.: Influence of loading history and soil type on the normal contact behavior of natural sand grain-elastomer composite interfaces. Polymers **13**, 1830 (2021). https://doi.org/10.3390/polym13111830
82. Mindlin, R.D.: Compliance of elastic bodies in contact. J. Appl. Mech. **16**, 259–268 (1949)
83. Hertz, H.: Über die Berührung fester elastischer Körper. Journal für die reine und angwendte Mathmatik **92**, 156–171 (1882)
84. Mindlin, R.D., Deresiewicz, H.: Elastic spheres in contact under varying oblique forces. J. Appl. Phy. **20**, 327–343 (1953)
85. Cheng, Z., Wang, J., Li, W.: The micro-mechanical behaviour of sand–rubber mixtures under shear: an experimental study based on X-ray micro-tomography. Soils Found **60**(5), 1251–1268 (2020)
86. Mollon, G.: Mixtures of hard and soft grains: micromechanical behavior at large strains. Granular Matter **20**(3), 1–16 (2018)
87. Zhang, J., Chen, X., Zhang, J., et al.: DEM investigation of macro- and micro-mechanical properties of rigid-grain and soft-chip mixtures. Particuology **55**, 128–139 (2021)
88. Mollon, G.: A multibody meshfree strategy for the simulation of highly deformable granular materials. Int. J. Numer. Meth. Eng. **108**(12), 1477–1497 (2016)
89. Nezamabadi, S., Nguyen, T.H., Delenne, J.Y., et al.: Modeling soft granular materials. Granular Matter **19**(1), 1–12 (2017)
90. Kasyap, S.S., Senetakis, K.: Interface load—displacement behaviour of sand grains coated with clayey powder: experimental and analytical studies. Soils Found **59**(6), 1695–1710 (2019)
91. He, H., Senetakis, K.: An experimental study on the micromechanical behavior of pumice. Acta Geotech. **14**(6), 1883–1904 (2019)
92. Sandeep, C.S., Marzulli, V., Cafaro, F., Senetakis, K., Pöschel, T.: Micromechanical behavior of DNA-1A Lunar regolith simulant in comparison to Ottawa sand. J Geophys Res Solid Earth **124**(8), 8077–8100 (2019)
93. Ren, J., He, H., Lau, K.C., Senetakis, K.: Influence of iron oxide coating on the tribological behavior of sand grain contacts. Acta Geotech (2022). https://doi.org/10.1007/s11440-021-01367-7
94. Duffaut, K., Landrø, M., Sollie, R.: Using Mindlin theory to model friction-dependent shear modulus in granular media. Geophysics **75**(3), E143–E152 (2010)